

# Experiments with a double solenoid system: Measurements of the ${}^6\text{He}+p$ Resonant Scattering

Rubén Pampa Condori

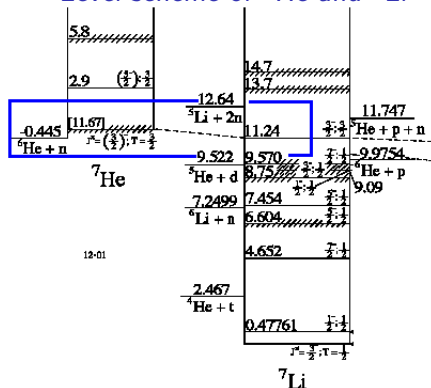
Institute of Physics - USP

2015

53. International Winter Meeting on Nuclear Physics  
26-30 January 2015, Bormio, Italy

# Introduction

## Level scheme of ${}^7\text{He}$ and ${}^7\text{Li}^1$

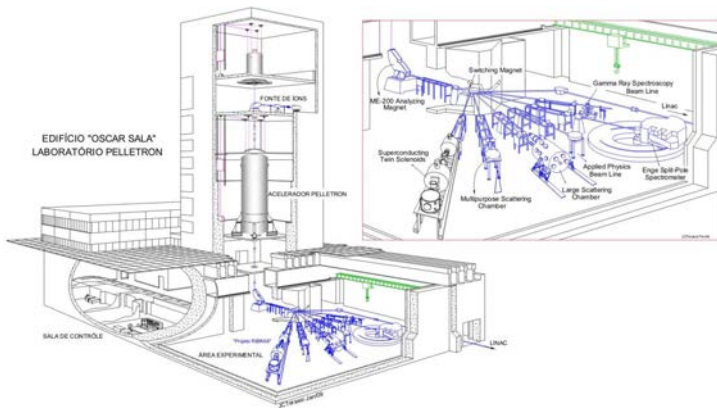


- Measurements focus in the region just above the threshold of fusion for the compound system  ${}^6\text{He} + p$ .
- Measurements of excitation functions of the  $p({}^6\text{He}, p){}^6\text{He}$  elastic scattering can provide information about the structure of the compound nucleus  ${}^7\text{Li}$
- We made these measurements to see the state 11.24 MeV  $3/2^-$   $T=3/2$  of the  ${}^7\text{Li}$  which is the IAS of the ground state of  ${}^7\text{He}$

<sup>1</sup>D.R. Tilley et al., Nucl. Phys. A 745, 155(2002)

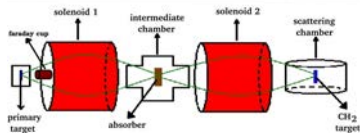
# Setup

## São Paulo Pelletron Laboratory



# Setup

## RIBRAS system

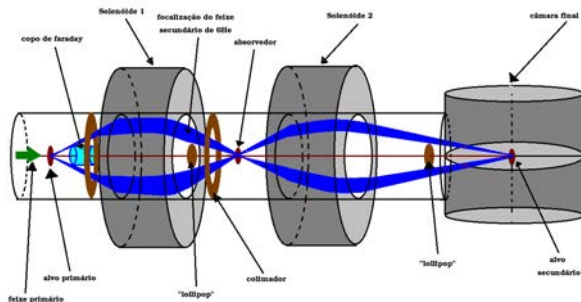


- We obtain the secondary  ${}^6\text{He}$  beam by the primary reaction  ${}^9\text{Be}({}^7\text{Li}, {}^6\text{He})$ .
- We used an absorber of polyethylene( $\text{CH}_2$ ) in the mid-scattering chamber.
- In the scattering chamber we used a thick target of polyethylene( $\text{CH}_2$ ) with thickness of  $12\text{mg}/\text{cm}^2$ .

## Radioactive Ion Beams in Brasil (RIBRAS)

# Setup

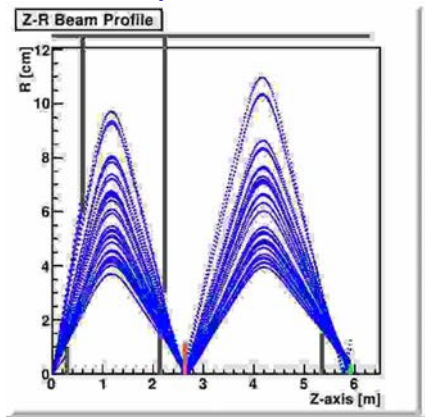
## RIBRAS system



The primary beam comes from the left side and the secondary particles are produced in the primary target by nuclear reactions. The standard primary target is a  $^9\text{Be}$  foil of 8-12 $\mu\text{m}$  thickness. The primary beam is suppressed by a Faraday cup, connected to a current integrator module which provides the total incident charge.

# Setup

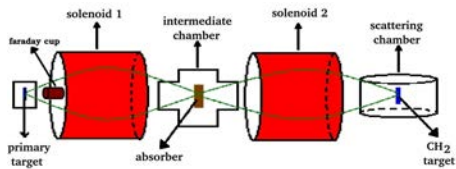
## RIBRAS system



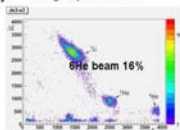
The first solenoid makes a  $B\rho = \frac{\sqrt{2mE}}{q^2}$  selection of the particles produced in the primary target. Particles with the same  $B\rho$  are focused in the ISO-250 intermediate scattering chamber and, unwanted particles are stopped by the collimators and blockers strategically positioned over the beam line.

# Setup

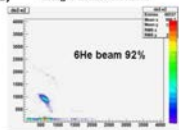
## RIBRAS system



(a) using only one solenoid

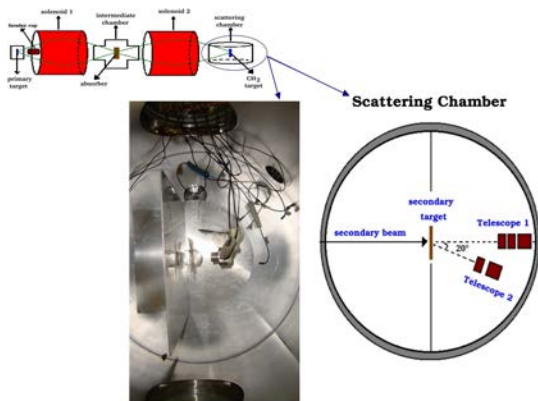


(b) using a double solenoid



Using a polyethylene foil as absorber in the mid-scattering chamber we improve the beam purity from 16% in the mid-scattering chamber to 92% in the secondary scattering chamber.

# Setup

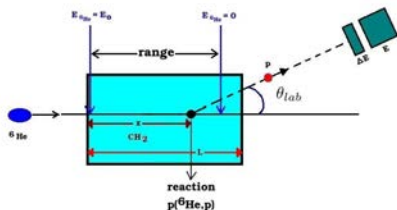


Two detectors were mounted in the scattering chamber.



## Thick Target Method

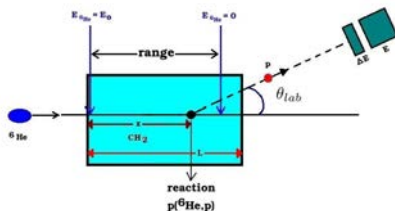
### Thick Target Method



- The thick target method, consists of using thick sheets of polyethylene  $\text{CH}_2$  to stop the secondary beam.
- The scattering can take place at any position in the  ${}^6\text{He}$  range and the energy of the recoil protons is related to the energy of the  ${}^6\text{He}$  particle at the scattering position.

## Thick Target Method

### Thick Target Method

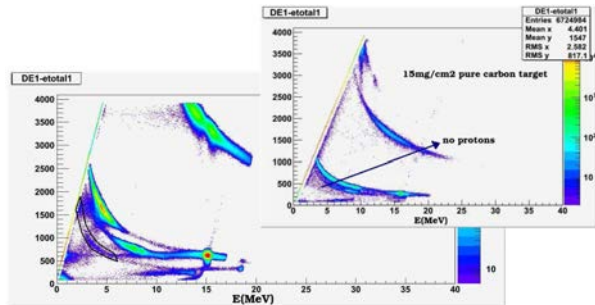


- So the reaction  $p({}^6\text{He},p)$  may happen in any point  $x$  of the  $\text{CH}_2$  target and the recoil protons have to travel a distance  $\frac{L-x}{\cos\theta_{\text{lab}}}$ .
- So the detected protons lose energy in the distance  $\frac{L-x}{\cos\theta_{\text{lab}}}$ , so this loss of energy is calculated and added to the energy of the detected protons.

To calculate this loss of energy we used the programs STOPX and KINEQ.

# Analysis

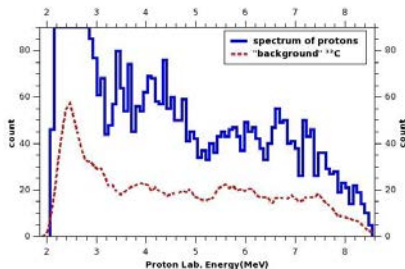
Spectrum measured with a  $\text{CH}_2$  ( $12\text{mg}/\text{cm}^2$ ) target at  $E_{\text{lab}}^{6\text{He}} = 12.2\text{MeV}$



We also conduct measurements with a pure carbon target intended to measure the effect which could cause the carbon present in the polyethylene target ( $\text{CH}_2$ ). As we can see in carbon target there is no line in the area corresponding to the proton.

# Analysis

Spectra measured with a  $\text{CH}_2(12\text{mg}/\text{cm}^2)$  target at  $E_{lab}^{6\text{He}} = 12.2\text{MeV}$



In this figure we can see the proton line projection into energy-axis. The contribution of the carbon is shown by the dashed curve in this spectrum. As we can see no peaks are seen in the region around the resonance peak in the carbon spectrum.

# Analysis

## Energy resolution

The energy resolution of 1MeV(FWHM) and intensity of 1000pps.

$$\Delta E_p = \Delta E_{6He} \left( \frac{dx}{dE} \right)_{6He} \left( \frac{dE}{dx} \right)_p$$

We know that:  $\frac{dE}{dx} \propto \frac{MZ^2}{E}$

$$\begin{aligned} \text{so: } \Delta E_p &= \Delta E_{6He} \frac{E_{6He}}{m_{6He} Z_{6He}^2} \frac{m_p Z_p^2}{E_p} \\ &\sim 90\text{KeV} \end{aligned}$$

(1)

# Analysis

From  $N_{cont}$  to  $\frac{d\sigma}{d\Omega}$

The experimental differential cross section  $d\sigma/d\Omega$  is given by:

$$\left(\frac{d\sigma}{d\Omega}\right)_{cm} = \frac{N_{cont} J}{\Delta\Omega N_{target} N_{beam}}$$

Where  $N_{target}$  is the number of scatterer nuclei inside the target per unit area

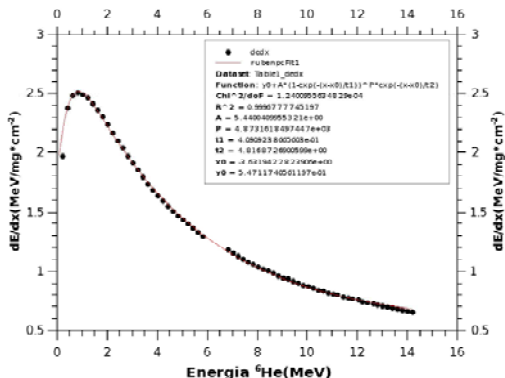
$N_{beam}$  is the total number of incident particles of the beam that hit the target

and  $\Delta E_{^6He}$  is the  $^6He$  energy step

$$N_{target} = \frac{\Delta E_{^6He}}{\frac{dE_{^6He}}{dx}}$$

# Analysis

## Stopping power of ${}^6\text{He}$ in $\text{CH}_2$

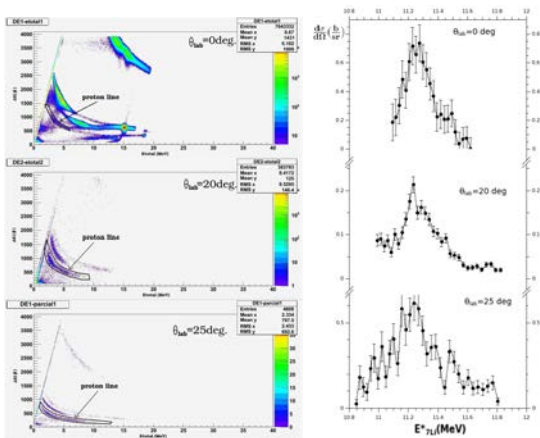


There was made a polynomial fit to these points ( $\frac{dE}{dx}$ ) obtained with the STOPX code.

# Analysis

Spectra measured with a  $\text{CH}_2$  (12mg/cm<sup>2</sup>) target at  $E_{lab}^{6\text{He}} = 11.5 - 12\text{MeV}$  and Excitation Functions

$$E_{7\text{Li}}^* = E_{cm} + Q_{fus}^{p+6\text{He}}$$

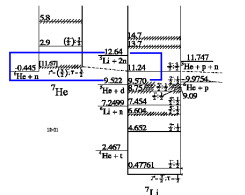




# Analysis

## Breit-Wigner function<sup>2</sup>

The spectra have been fitted by a Breit-Wigner function (2) folded with a gaussian whose width is the experimental resolution  $\sigma_{c.m.}^{exp. res.} = 90\text{keV}$ (3).



88 D.R. Tilley et al. / Nuclear Physics A 708 (2002) 3–263

Table 7.2  
Energy levels of  ${}^7\text{Li}$

$E_x$ (MeV $\pm$ keV)	$J^\pi$ ; $T$	$t_{1/2}$ or $T_{1/2}$ (keV)	Decay	Reactions
g.s.	$\frac{3}{2}^+$		stable	1, 2, 3, 5, 6, 7 18, 20, 21, 22
11.24 $\pm$ 30	$\frac{7}{2}^-$	260 $\pm$ 35	n, p	6, 9, 39
13.7	$\approx 500$		n	15
14.7 <sup>a</sup>	$\approx 700$		n	15

$$L(E) = \frac{N\Gamma(E, \ell)}{(E - E_r)^2 + \frac{\Gamma(E, \ell)^2}{4}} \quad (2)$$

$$L_c(E) = \int dE' L(E') e^{\frac{-(E-E')^2}{2\sigma_{res}^2}} \quad (3)$$

$\theta_{lab}$	$N = \gamma_p^2$	$\Gamma(\text{keV})$	$E_r(\text{MeV})$
$0^\circ$	$0.052 \pm 0.004$	$254 \pm 24$	$11.11 \pm 0.02$
$20^\circ$	$0.011 \pm 0.001$	$262 \pm 25$	$11.28 \pm 0.02$
$25^\circ$	$0.036 \pm 0.001$	$256 \pm 27$	$11.11 \pm 0.03$

<sup>2</sup>The fit was performed using the program XFIT developed by Guilherme Amadio

(<http://www.cecm.usp.br/~amadio/aboutme>)

# Analysis

R-matrix calculations-Excitation Functions  $E_{\gamma Li}^* = E_{cm} + Q_{fus}^{p+{}^6He}$

We have also performed R-matrix calculation considering two decays channels: (p,p) and (p,n)

The latter measured by Rogachev et al.

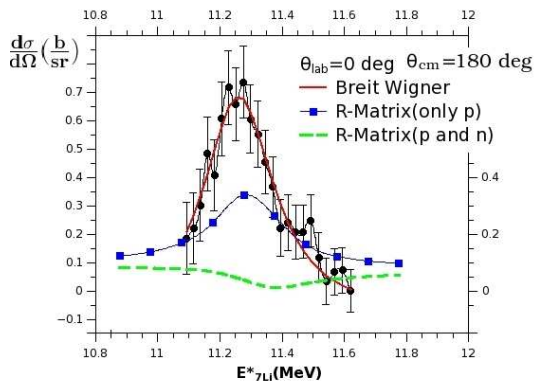


$$\frac{\Gamma_p}{\Gamma} \approx 0.2 \text{ and } \frac{\Gamma_n}{\Gamma} \approx 0.8 \left\{ \begin{array}{l} \frac{\gamma_p^2}{\gamma_n^2} = 2 \\ \Gamma = \Gamma_p + \Gamma_n = 0.265 \text{ MeV} \\ = 2\gamma_p^2 P_\ell(E_R) + 2\gamma_n^2 P_\ell(E_R - Q) = 0.265 \text{ MeV} \end{array} \right.$$

3 Calculations have been performed by P.Descouvemont.

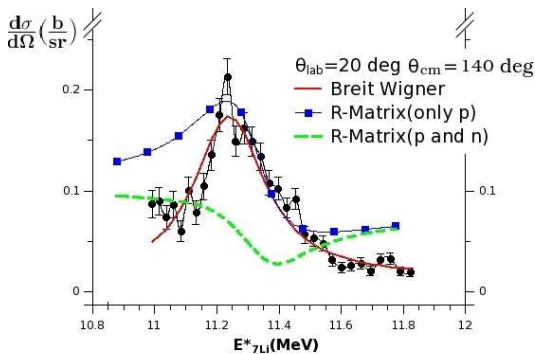
# Analysis

R-matrix calculations-Excitation Functions  $E_{7Li}^* = E_{cm} + Q_{fus}^{p+{}^6He}$



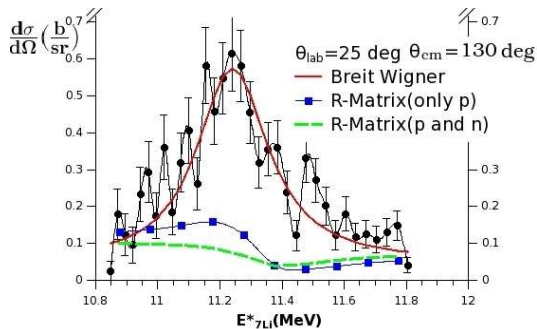
# Analysis

R-matrix calculations-Excitation Functions  $E_{7Li}^* = E_{cm} + Q_{fus}^{p+{}^6He}$



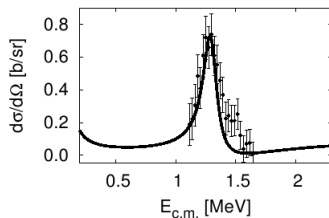
# Analysis

R-matrix calculations-Excitation Functions  $E_{7Li}^* = E_{cm} + Q_{fus}^{p+{}^6He}$



# MCAS calculation

## Multichannel Algebraic Scattering Approach<sup>4</sup>



- L. Canton et al. PoS(X LASNPA) 047.
- K. Amos et al. Nucl. Phys. A 728, 65 (2003).
- K. Amos et al, Nucl. Phys. A912, 7 (2013).
- K. Amos et al, Nucl. Phys. A 879, 132 (2012).

- S. Karataglidis et al, Nucl. Phys. A 813, 235 (2008).

The multi-channel algebraic scattering (MCAS) method solves the coupled-channel Lippmann- Schwinger LS equations describing a two-cluster system, in both bound-state sub-thresholds and scattering regimes.

<sup>4</sup> Calculations have been performed by L. Canton.

# Summary

- We measured the  $p(^6\text{He},p)^6\text{He}$  elastic scattering excitation function at three angles  $\theta_{lab}^{proton}=0, 20$  and  $25$  degrees. We clearly see peaks in the position corresponding to the  $11.24\text{MeV}$ , state of the  $^7\text{Li}$ .
- A fit of the proton spectrum using a Breit- Wigner function shows that the peak has the expected energy and width at the three angles.
- R-matrix calculations give results that are in contradiction with the data. Reasonable results are obtained for the  $(p,p)$  one channel R-matrix calculation. In this calculation we have used the partial widths reported in Rogachev et al. for the  $(p,p)$  and  $(p,n)$  channel.

## What next?

We will work with three telescopes at  $\theta_{lab} = 0, 25, 45$  degrees (which corresponding to  $\theta_{cm} = 180, 130, 90$  degrees) to obtain the three excitation functions in one run. In this way we will be sure that the three angles correspond to the same  $N_{beam}$  and we will have an angular distribution. This was not the case in the previous experiment when the measurement a 25degrees was taken with a different run.



# RIBRAS collaboration

- Universidade de São Paulo - IFUSP  
A. Lépine-Szily, R. Lichtenthäler, V. Guimaraes, L. Gasques, P. N. de Faria, K.C.C. Pires, V. Scarduelli, M.C. Morais, R. Pampa Condori, E. Leistenschneider, E. Benjamim, O. Camargo Jr. J.Alcantara-Nunez, E. Crema, Y. Otani, M.S. Hussein
- Universidade Federal Fluminense (UFF)  
P.R.S. Gomes, J. Lubian, J.M.B. Shorto, D.S. Monteiro, D. R. Mendes, V. Morcelle
- Université Libre de Bruxelles, Brussels, Belgium  
P. Descouvemont
- Laboratorio Tandar, Buenos Aires, Argentina  
A. Arazi
- Universidad de Sevilla, Espanha  
A.M. Moro, M. Rodríguez-Gallardo
- University of Notre Dame, EUA  
J. Kolata

# Thanks for your attention!

Financial Support:

